Applied Catalysis B: Environmental 111–112 (2012) 178–184

Contents lists available at SciVerse ScienceDirect

Applied Catalysis B: Environmental

journal homepage: www.elsevier.com/locate/apcatb

Improved dehydrogenation of ammonia borane over Co-P-B coating on Ni: A single catalyst for both hydrolysis and thermolysis

N. Patel*, A. Kale, A. Miotello

Dipartimento di Fisica, Università degli Studi di Trento, I-38123 Povo (Trento), Italy

ARTICLE INFO

Article history:
Received 5 May 2011
Received in revised form 23 August 2011
Accepted 25 September 2011
Available online 29 September 2011

Keywords:
Hydrogen generation
Ammonia borane
Co-P-B coating
Electroless deposition
Thermolysis
Hydrolysis

ABSTRACT

Co-P-B catalyst coatings have been synthesized on Ni-foam by using electroless deposition (ED) and their catalytic activity was investigated by catalytic dehydrogenation of ammonia borane (AB, NH_3BH_3) for H_2 generation. Co-P-B catalyst (both in form of powder and coating) showed superior catalytic activity in hydrolysis reaction of AB than that of Co-B powder, with complete evolution of H_2 (97%) at very high rate (2 l/min/g catalyst). This was mainly attributed to synergic effect caused by B and P over Co active sites to lower the activation energy of the process. For thermolysis reaction, it was observed that AB loaded on Co-P-B/Ni catalyst releases first mole of H_2 at considerably low temperature starting at 50 °C and with desorption peak centered at 80 °C. To our knowledge this value is the lowest reported for solid state catalyst. Moreover, the catalytic thermolysis did not present any induction time and minimizes the formation of undesirable byproduct like borazine and ammonia. The present result suggests that Co-P-B coated on Ni is a highly efficient and low cost catalyst and can be used for both hydrolysis as well as thermolysis reaction of NH_3BH_3 with the important advantage that it can be easily recovered and repeatedly reused.

1. Introduction

Hydrogen has emerged as a sustainable energy carrier while avoiding emission of greenhouse gases and thus mitigating problems related to climatic change. However, for a real clean hydrogen-based technology it is essential to develop safe and convenient hydrogen storage and on-board production systems. Although in the past considerable efforts have been focused on hydrogen storage materials, major challenges concerning gravimetric and/or volumetric efficiency still remain [1].

Chemical hydride such as ammonia borane (AB, NH_3BH_3) is a leading candidate as a storage medium with potential capacity of 19.6 wt% H_2 [2]. Dehydrogenation of AB can be carried out by either hydrolysis in solution form or by thermolysis reaction in solid state. The major advantage with hydrolysis reaction is that it takes place at room temperature, but solubility limit of AB in water leads to the practical storage capacity less than 5 wt% H_2 [3]. Therefore, the aqueous solution of AB can only be attractive for the off-board portable application. In addition, the catalyst material is required to initiate the hydrolysis reaction by lowering the kinetic barrier as well as to accelerate the H_2 generation in a controllable manner. On the contrary, thermolysis of AB takes place in solid state at elevated temperatures and seems to be more practical for on-board applications owing to the high hydrogen storage capacity. However, its practical application is seriously hindered due to three major requirements that have yet to be achieved: (1) reduction of dehydrogenation temperature below 85 °C which is the operating temperature of fuel cell, (2) improving the H_2 release kinetics at this temperature, and (3) volatile byproduct (borazine and ammonia) formation must be inhibited. The single solution to overcome all these barriers is to develop efficient and low cost catalysts to enhance kinetics of the reactions, to lower thermodynamic stability under moderate temperature conditions, and by following different reaction routes to prevent the borazine formation.

Noble catalysts like Pt, Rh, and Ru supported on Al_2O_3 [4], C [5,6] and TiO_2 [7], K_2Pt_6Pt [8], and nanoclusters of Pd (0) [9], Ru (0) [10] and Rh (0) [11] have been utilized in the past to enhance the hydrogen production rate by hydrolysis of AB. However, these catalysts do not seem to be viable for industrial application considering their cost and availability. Transition metals such as Co supported on Al_2O_3, SiO_2 [12], and C [13], Co (0) [14–16], Ni (0) [17] and Fe (0) [18] nanoclusters, Ni based alloy [19], and Ni–SiO_2 nanospheres [20] are generally used to accelerate the hydrolysis reaction of NH_3BH_3. For thermolysis reaction, catalysts for example silica nanoscaffold [21], metal-organic framework [22], ionic liquid [23], carbon cryogel [24], boron nitride [25], metals (Li, Ru, Rh, Cu and Ni) [26–28] and polymers [29] were used in past to improve the H_2 generation

* Corresponding author.
E-mail address: patel@science.unitn.it (N. Patel).

0926-3373/$ – see front matter © 2011 Elsevier B.V. All rights reserved.
doi:10.1016/j.apcatb.2011.09.032

kinetics at moderate temperature. Few of these catalysts were also successful in eliminating volatile byproduct formation. Nevertheless, it is required to develop a single catalyst for both hydrolysis as well as thermolysis reaction because AB, with appropriate catalyst, can either be directly added to water or submitted to temperature to efficiently produce hydrogen. Cheng et al. [30] used NiPt alloy hollow sphere catalyst for both the dehydrogenation reactions. However, high cost and scarcity of this precious metal make it necessary to explore new routes to replace them with non-noble catalysts. Cobalt based alloys (Co–B [31], Co–Cr–B [32], Co–Ni–B [33], Co–P–B [34], and Co–Ni–P–B [35]) are considered to be good candidates owing to their relevant catalytic activity, low cost, and ease to synthesize. Generally, most of the catalysts are used in form of homogeneous powders which, however, have limitations related to separation and aggregation during the reaction. On the other hand, catalysts in form of thin film (or coating) not only have generally better catalytic properties due to their surface morphology and structure but also they can be easily recovered and reused thus being very suitable tool to act as on/off switch for generation of H_2 [36].

In this paper we report on the synthesis of Co-P-B catalysts in form of thin coating on Ni-foam by using electroless deposition (ED) and investigate the hydrogen production process through catalytic hydrolysis and thermolysis of AB. The kinetics is studied as function of both AB concentration and reaction temperature. For hydrolysis reaction, the catalyst coating showed excellent catalytic activity to produce expected amount of H_2 with high rate (~2020 ml/min/g catalyst) mainly attributed to synergic effect caused by P and B elements over Co active sites. For thermolysis reaction, in presence of Co-P-B catalyst coating, the dehydrogenation temperature of AB was reduced to 80 °C for the release of first mole of H_2 with increment in release rate by factor of 5. The borazine evolution was also significantly minimized.

2. Experimental

Co-P-B coatings were deposited by using electroless deposition method. Ni-foam (Inco Co. LTD, density = 380 g/m^2, pore size = 590 μm, thickness = 1.7 mm) was selected as support for catalyst coatings because of its high surface area provided by the intrinsic porous structure. Specimen (2 cm × 1 cm) of Ni-foam was ultrasonically cleaned with acetone followed by NaOH solution (1 M) to remove soaks, lubricants, and finger prints. The surface of specimen was deoxidized and activated by dipping in HCl solution (30% concentrated) for 2 min and then washed with distilled water and dried at 323 K in N_2 atmosphere. This pretreated Ni-foam specimen was immersed in 10 ml of aqueous solution containing 0.1 M of cobalt salt ($CoCl_2$) and sodium hypophosphite (NaH_2PO_2) for 1 min at room temperature under stirring. Then equal volume of sodium borohydride ($NaBH_4$) solution (0.25 M), used as a reducing agent, was poured in the previous solution. The Ni foam was removed from the mixture after bubble generation ceased. The previous immersion step was repeated 4 times in order to completely cover (as specifically proved by scanning electron microscopy analysis, see below) the Ni foam support. Finally the Ni foam was extensively washed with distilled water and ethanol before drying at around 323 K under continuous N_2 flow. The molar ratio of (P + B)/Co and B/P was kept 4 and 2.5 in the Co-P-B catalyst, respectively, because at this value we previously obtained maximum H_2 generation rate by hydrolysis of $NaBH_4$ [34]. The weight of Co-P-B coating was evaluated by measuring the weight of Ni foam specimen before and after deposition. For comparison, Co-P-B powder catalyst with similar molar ratio as in case of coating, was also synthesized by adding $NaBH_4$ to an aqueous solution containing $CoCl_2$ and NaH_2PO_2 under vigorous stirring. The black powder separated from the solution during reaction course was filtered and then extensively washed with distilled water and ethanol before drying at around 323 K under continuous N_2 flow. Similarly, Co-B powder catalyst was also synthesized in absence of NaH_2PO_2.

The surface morphology of all catalysts was studied by scanning electron microscope (SEM-FEG, JSM 7001F, JEOL) equipped with energy-dispersive spectroscopy analysis (EDS, INCA PentaFET-x3) to determine the composition of the samples. Structural characterization of the catalyst powders was carried out by conventional X-ray diffraction (XRD) using the Cu K_α radiation (λ = 1.5414 Å) in Bragg–Brentano (θ–2θ) configuration. Studies of surface electronic states and composition of the catalysts were carried out using X-ray photoelectron spectroscopy (XPS). X-ray photoelectron spectra were acquired using a SCIENTA ESCA200 instrument equipped with a monochromatic Al K_α (1486.6 eV) X-ray source and a hemispherical analyzer. No electrical charge compensation was necessary to perform the analysis.

For catalytic hydrolysis measurements, a solution of AB (Sigma Aldrich) with 0.025 M was prepared. The generated hydrogen quantity was measured through a gas volumetric method in an appropriate reaction chamber with thermostatic bath, wherein the temperature was kept constant within accuracy of ±0.1 K. The chamber was equipped with pressure sensor, stirrer system, catalyst insertion device, and also coupled with an electronic precision balance to accurately measure the weight of water displaced by the hydrogen produced during the reaction course. A detailed description of the measurement apparatus is reported in Ref. [37]. In all the runs, the catalyst was placed on the appropriate device inside the reaction chamber and the system was sealed. Catalyst powder or coating (10 mg) was added to 150 ml of the above AB solution, at 298 K, under continuous stirring. In order to make comparison, the stoichiometric hydrogen cumulative production yield (%) versus time was plotted instead of the hydrogen volume (ml) versus time. The efficiency of the catalyst coating was compared with the corresponding powder by using analogous amount of catalyst (10 mg).

For catalytic thermolysis reaction, Co-P-B catalyst deposited over Ni foam by ED (henceforth this catalyst is designated as Co-P-B/Ni) was dipped in two different solutions of NH_3BH_3 (1.0 M) with methanol (MeOH) or tetrahydrofuran (THF) for 3 min to incorporate AB layer over catalyst coating. The solution over the catalyst surface was later dried under vacuum condition for 5 min at room temperature. These steps of dipping and drying were repeated several times in order to completely cover the Co-P-B catalyst over Ni foam with AB. The weight ratio of Co-P-B catalyst to AB was always kept approximately to 1:7. The samples were later maintained in vacuum condition overnight to remove any organic solvents. The thermal decomposition of NH_3BH_3 was monitored by temperature programmed desorption spectroscopy (TPDS) system. TPDS analysis was performed, in an ultra high vacuum chamber, by heating the sample in a linear temperature ramp (2 °C/min.) and measuring the mass signal of desorbed gases by a quadrupole mass spectrometer (QMS) equipped with a secondary electron multiplier [38]. Fourier transform infrared spectroscopy (FTIR) was used to detect AB over Ni foam. The measurements were carried out over sample pellets, made with KBr, in absorbance mode at normal incidence in the spectral range between 4000 and 400 cm^{-1} using a Bruker (Equinox 55) spectrometer at room temperature. The volume of H_2 gas evolved during the thermolysis reaction was measured by water displacement method. The flask containing Co-P-B/Ni catalyst covered with AB (70 mg) was immersed in a mineral oil bath heated at set temperature. Thermocouple was placed over the catalyst surface to accurately measure the temperature. The volume of the gas was evaluated by accurately measuring the weight of water displaced by the hydrogen produced during the reaction course.

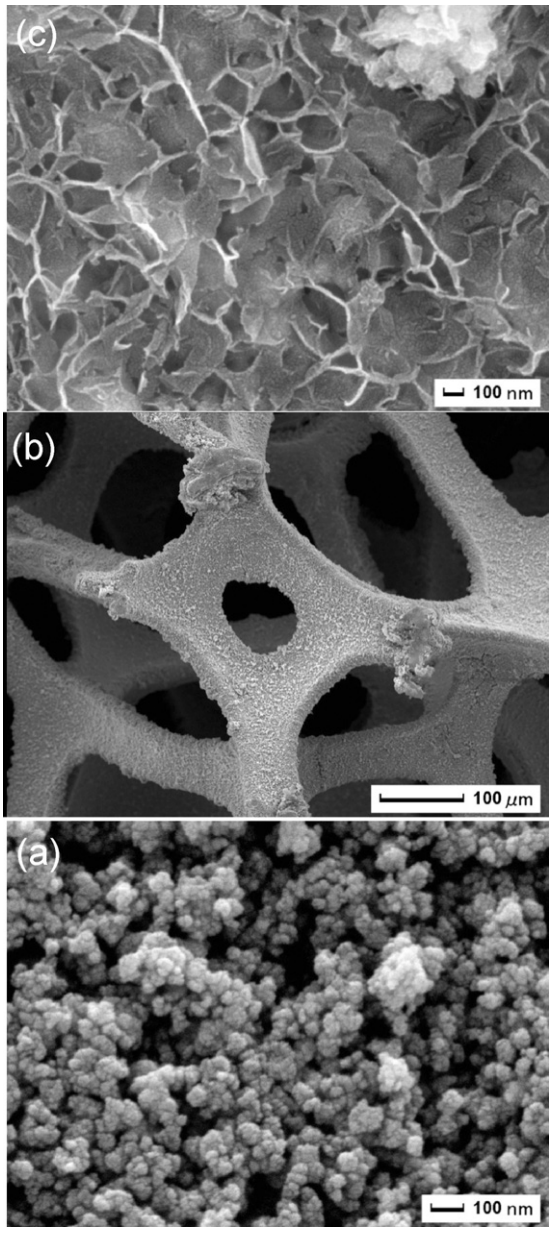

Fig. 1. SEM micrographs of (a) Co-P-B powder and corresponding coatings synthesized by ED on Ni foam at (b) low magnification and (c) high magnification.

3. Results and discussion

In our previous work [34], we have synthesized and analyzed Co-B, Co-P, and Co-P-B catalyst powders for hydrogen generation by catalytic hydrolysis of $NaBH_4$. We found that ternary alloy catalyst in form of Co-P-B was able to produce hydrogen with much higher rate as compared to the binary alloys Co-P and Co-B [34]. Later this Co-P-B catalyst was coated on porous Ni foam to have the additional advantage to be recovered and reused several times for the catalysis reaction [39]. In present work, this Co-P-B catalyst coated over Ni foam was tested for the catalytic hydrolysis and thermolysis of AB.

Structural characterization by XRD showed that the Co-P-B catalyst powder and their corresponding coating synthesized by ED were amorphous in nature (figure not shown). The diffraction spectra indicate short-range order and long-range disorder and both these features might contribute to enhance the catalytic activity [40]. In Fig. 1(a) we present SEM images of Co-P-B catalyst powder which shows particle-like morphology with particles having spherical shape and average size in the range of 30–40 nm. During catalyst preparation, an efficient reducing agent in form of $NaBH_4$ was utilized which is able to cause the rapid reduction of Co ions that avoid particles growth above a few nanometers. However, because of the high surface energy related to these particles, they tend to agglomerate as observed in the SEM image (Fig. 1(a)). In our previous work [39], we have made several ED deposition steps of Co-P-B on Ni foam and found that a single step is not enough to completely cover the surface of the Ni foam. At least 3–4 deposition steps are necessary to make complete coverage, while by making more than 4 deposition steps only the weight of the catalyst coating increases. Hence, we made 4 deposition steps of Co-P-B to completely cover the Ni foam as seen in Fig. 1(b). Surface morphology of the Co-P-B coating (Fig. 1(c)) on Ni-foam at higher magnification shows two-dimensional nano-flakes like structure with space separation of a few tens to hundreds of nanometers. The surface of Ni-foam might act as a nucleation sites for the Co-P-B catalyst thus favoring the final observed peculiar structure.

Fig. 2(a) reports the XPS spectra in $Co2p_{3/2}$ level of Co-B powder and Co-P-B catalyst coating where two peaks appear with binding energies of 778.4 and 781.6 eV indicating that Co metal exists in both elemental and oxidized states respectively. The peaks due to oxidized Co are mainly present in form of +2 state attributed to $Co(OH)_2$, which would have been formed during catalyst preparation [41,42] or when it was exposed to ambient atmosphere. This cobalt hydroxide ($Co(OH)_2$) does not cause major negative effects on catalytic activity because it can be easily reduced by chemical hydrides in the course of the hydrolysis forming catalytically active phase [43]. The amount of $Co(OH)_2$ is minimum in Co-P-B catalyst as compared to Co-B. Two XPS peaks with binding energy (BE) of 188.2 eV and 192.1 eV were also observed for the B1s level in Co-P-B catalyst (Fig. 2(b)), which are assigned to elemental and oxidized boron respectively [41]. By comparing the BE of pure boron (187.1 eV) [44] with that of the elemental boron in the catalyst, one observe a positive shift of 1.1 eV. This shift indicates that there may be an electron transfer from alloying B to vacant d-orbital of metallic Co which makes B electron deficient and Co enriched with electrons. These electron-enriched metal active sites repel the adsorption of oxygen atoms from the ambient atmosphere, while they are strongly adsorbed by the electron-deficient B. In other words, alloying B oxidizes itself to effectively protect metals from oxidation in ambient condition [45] which is also the case in the Co-B catalyst [34]. In the P2p level (Fig. 2(c)), two kinds of phosphorous species appear on Co-P-B catalyst with binding energy of 130 eV and 133.3 eV. The lower BE is attributed to the metallic phosphorous while the higher BE is assigned to oxidized phosphorous. No significant shift in BE of metallic phosphorous was observed with respect to the elemental one, indicating that the electron transfer between Co and P in Co-P-B could be neglected. The surface atomic composition, calculated from XPS spectra, shows that the amount of the surface Co sites is higher for Co-P-B (Co ~70 at.%) as compared to Co-B (Co ~60 at.%) catalyst. This shows that phosphorus plays some role to favor the enrichment of the catalyst surface with Co sites. This result reveals that the role of P in the Co-P-B catalyst is to favor the enrichment of the surface with Co active sites.

The catalytic behavior of Co-P-B coating, synthesized by ED, was compared with that of the Co-P-B and Co-B powder for hydrolysis of AB. Hydrogen generation yield was measured, as a function of time, during the hydrolysis of AB solution (0.025 M) in presence of Co-B and Co-P-B powder and of Co-P-B/Ni coating at 298 K (Fig. 3). The figure clearly shows that all the catalysts are active and produce hydrogen instantaneously as soon as they come in contact with the AB solution. Co-P-B catalyst in form of powder and coating showed almost similar catalytic activity for hydrolysis reaction. Similar results were obtained for hydrolysis of $NaBH_4$ using same composition of the Co-P-B catalyst [39]. However, the Co-P-B

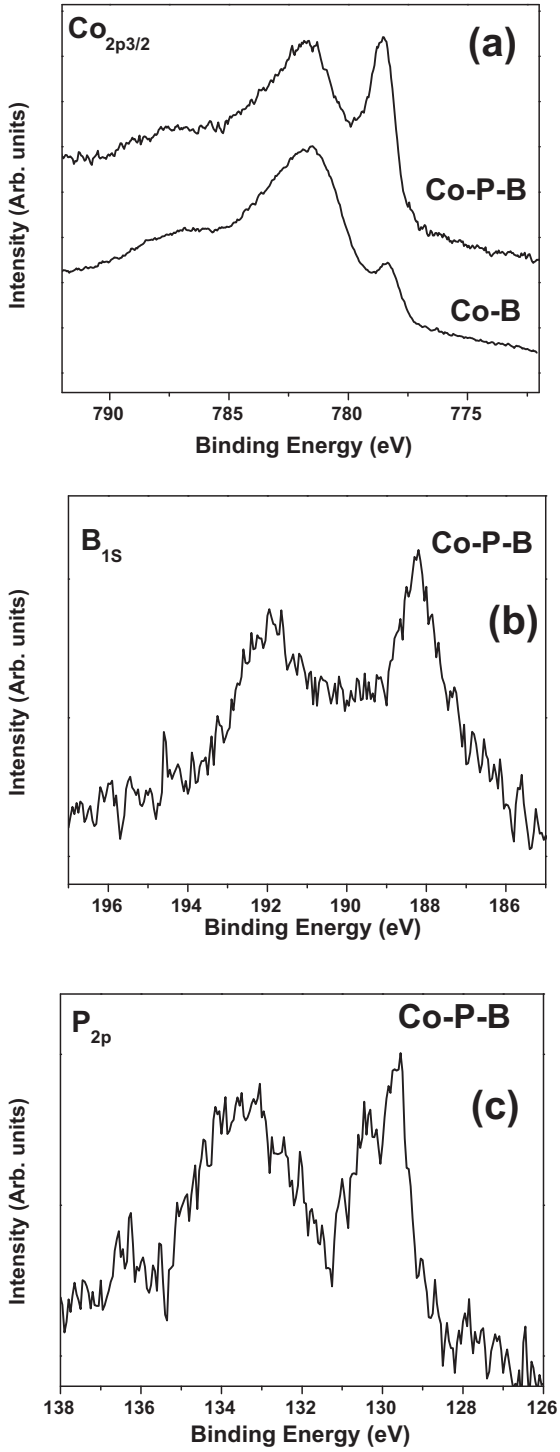

Fig. 2. X-ray photoelectron spectra of $Co2p_{3/2}$, P2p, and B1s level for Co-P-B (B/P molar ratio = 2.5) catalyst and $Co2p_{3/2}$ level for Co-B catalyst.

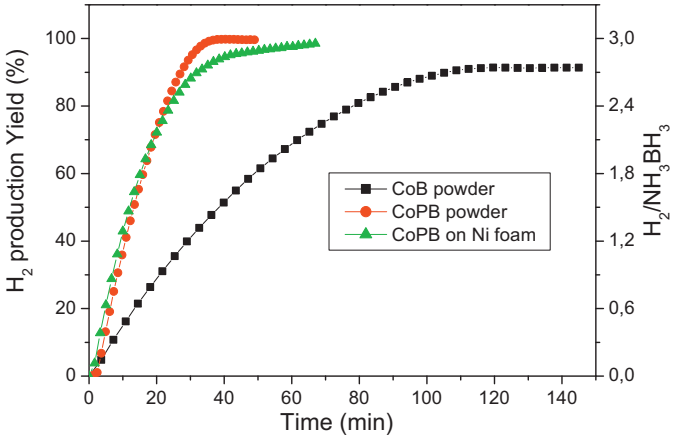

Fig. 3. Hydrogen generation yield as a function of reaction time obtained by hydrolysis of NH_3BH_3 (0.025 M) with Co-B and Co-P-B powders and Co-P-B coating synthesized on Ni substrate by ED.

catalyst (both powder and coating) exhibits much higher catalytic activity as compared to the Co-B powder and it was able to complete the reaction within ~36 min while the same amount of Co-B powder catalyst (~10 mg) took about ~140 min. The total amount of hydrogen generated by hydrolysis of AB using Co-P-B catalyst (H_2/NH_3BH_3 = 2.95) is closer to the quantitative yield, expected from the reaction stoichiometry (H_2/NH_3BH_3 = 3.0), than that generated by Co-B powder (H_2/NH_3BH_3 = 2.65). During the reaction course the catalyst coating was very stable and remained intact over Ni-foam even under vigorous hydrogen production (as observed by SEM). The enhanced catalytic activity for Co-P-B catalyst during hydrolysis of AB is mainly attributed to synergistic effects occurring from the alloying P and B. The role of former element is to create high number of Co active sites on the surface while the later element provides the necessary electron density to Co active sites for the catalytic activity and at a same time protects Co against oxidation. The maximum H_2 generation rate obtained with the same catalyst amount (10 mg) by using the Co-P-B coating and powder (~2020 ml/min/g catalyst) has been found 5 times higher than that obtained using the Co-B powder (~400 ml/min/g catalyst) proving a better catalytic performance due to synergic effects caused by P and B elements as previously underlined. This result also indicates that the Co-P-B catalyst both in powder form as well as coated on Ni foam shows good activity.

The H_2 generation yield values for Co-B powder reported in Fig. 3 were perfectly fitted by using a single exponential function suggesting that hydrolysis catalyzed by Co-B powder is a first order kinetic process with respect to AB. Importantly, the H_2 generation data produced with Co-P-B catalyst were fitted linearly thus showing a zero order kinetic process with respect to AB concentration. This was also confirmed by measuring the H_2 generated volume from hydrolysis of AB by using 4 different concentration values of AB, namely: 0.025, 0.050, 0.10, and 0.15 M in the starting solution by keeping the amount of Co-P-B catalyst on Ni foam constant at 10 mg. The results are reported in Fig. 4. In the inset of Fig. 4 we report the plot of ln (rate) versus ln (concentration of AB) which is fitted linearly with positive slope of 0.11: the nearly zero value of the slope proves the zero order kinetics with respect to the NH_3BH_3 concentration. The highly catalytic active Co sites on catalyst surface, caused by the synergic effect of P and B, are able to confine the hydrogen generation to a surface reaction. Similar zero order kinetics with respect to AB concentration was proposed by Xu and Chandra [13] ($Co/\gamma\text{-}Al_2O_3$), Yao et al. [19] (NiAg alloy catalyst), and Özkar and co-workers [9] (Ru and Pd nanoclusters). On the contrary, the first order kinetics involving diffusion of BH_3^- on the catalyst surface is the rate limiting step in the case of Co-B powder.

In Fig. 5, the H_2 generation yield, obtained through hydrolysis of AB (0.025 M) solution using Co-P-B/Ni catalyst is reported as a function of time at different reaction temperatures. The Arrhenius plot of the hydrogen production rate (inset of Fig. 5) gives an activation energy value of about 39 ± 1 kJ mol^{-1} for Co-P-B coating which is lower than that obtained with Co-B powder (44 ± 1 kJ mol^{-1}) [46]. This value is also much lower than that reported in the literature when using noble metal catalysts like Ru (47 kJ mol^{-1}) [10] and Rh nanoclusters (67 kJ mol^{-1}) [11], Pd metal (44 kJ mol^{-1}) [9],

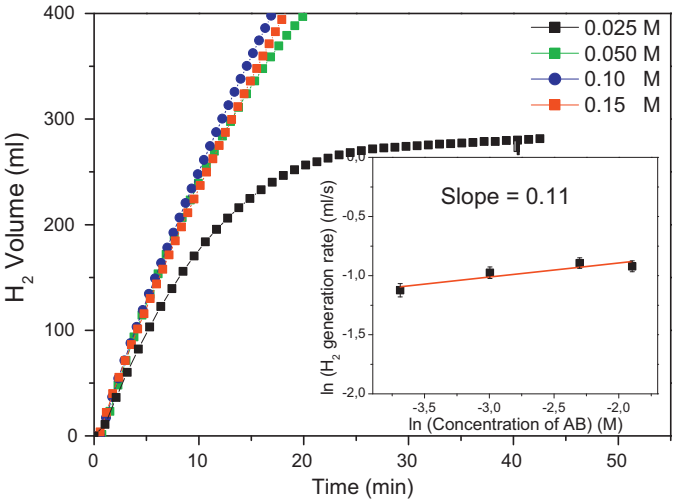

Fig. 4. Hydrogen generated volume, as a function of reaction time, with Co-P-B/Ni catalyst coating obtained by hydrolysis of NH_3BH_3 solution with 4 different concentrations of NH_3BH_3 ranging from 0.025 to 0.15 M. Inset shows the plot of ln (H_2) generation rate versus ln (concentration of NH_3BH_3) to determine the kinetic reaction order with respect to AB.

Ru/C (76 kJ mol^{-1}) [6], and K_2PtCl_6 (86 kJ mol^{-1}) [8]. The activation energy value obtained in the present case is also lower than that obtained by other catalysts such as NiAg (51.5 kJ mol^{-1}) [19], Co/γ-Al_2O_3 (62 kJ mol^{-1}) [13], Co-Mo-B/Ni foam (44 kJ mol^{-1}) [47], and Co (0) nanoclusters (46 kJ mol^{-1}) [14]. The favorable activation energy value obtained in the present work is again an evidence of the synergetic effects of P and B in Co-P-B to enhance the catalytic reaction.

Co-P-B/Ni exhibits very good activity for hydrolysis of AB with the possible important advantage to be recovered and reused several times: for this reason we further test its catalytic performance in the thermolysis of AB. Several strategies have been adopted in the past to load AB over solid catalyst by either soaking or dipping in AB solution made with either THF or alcohol (methanol, ethanol etc.) [21,22,24,30]. Thus, in order to study the effect of solvent over the AB loading we prepared two set of samples by dipping the composite catalyst coating in AB solution (1 M) of either THF or MeOH. The AB deposited over Co-P-B coating was in form of particles so measuring the thickness of AB layer was not possible.

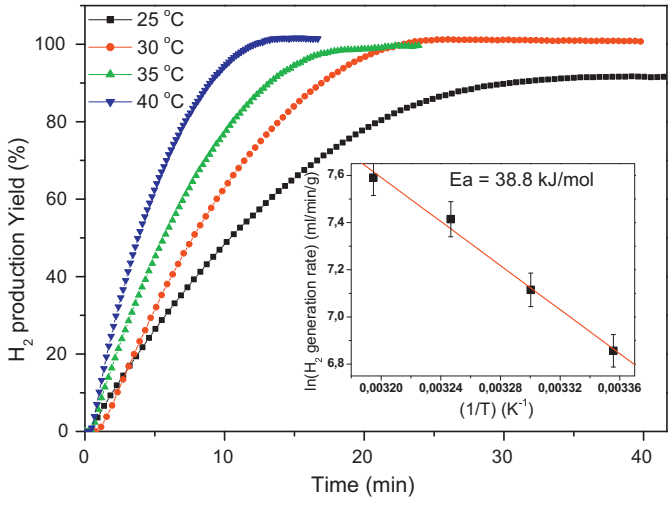

Fig. 5. Hydrogen generation yield as a function of reaction time by hydrolysis of NH_3BH_3 (0.025 M) solution with Co-P-B/Ni catalyst coating measured at 4 different solution temperatures. Inset shows the Arrhenius plot of the H_2 generation rates.

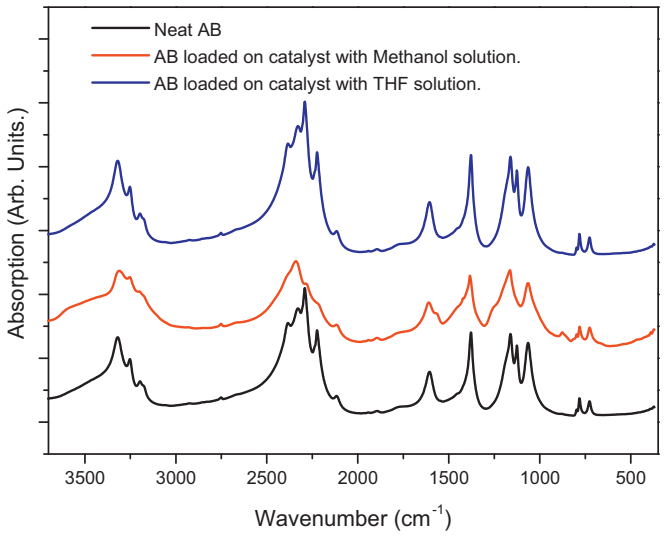

Fig. 6. FTIR spectra of neat AB powder and AB loaded over Co-P-B/Ni catalyst by using THF and MeOH based solution.

During SEM imaging, the energetic electron beam decomposes the AB molecule causing liberation of H_2 gas from the AB surface thus it is difficult to maintain the vacuum in the system to acquire the SEM image. To confirm that the white powder deposited on catalyst is AB we performed FTIR measurement on KBr pellets samples with AB powder scratched from the Co-P-B/Ni catalyst. Fig. 6 represents the FTIR spectra of neat AB powder and of AB loaded by using THF or MeOH solution. In neat AB, the absorbance bands centered at 3320, 1605, and 1350 cm^{-1} attributed to N–H vibration modes of stretching, bending, and rocking, respectively, are clearly visible [24]. The bands centered at 2290 (2225) cm^{-1} and 1130 (1070) cm^{-1} are assigned to B–H vibration modes of stretching and bending, respectively [24]. The band at 785 (729) cm^{-1} is due to B–N stretching vibration mode [24]. The AB loaded by using THF solution shows all the absorbance bands of B–H, B–N, and N–H similar to that observed for neat AB. For AB samples loaded by using MeOH solution, the peaks due to B–H vibration are either disappeared (1130 and 2225 cm^{-1}) or its relative intensity was decreased (1070 and 2290 cm^{-1}). This result shows that pure AB is coated on Ni foam with THF solution while the Co-P-B catalyst in MeOH solution of AB initiates the methanolysis reaction to break the B–H bond and causing the H_2 gas production. Indeed we have observed bubbles formation when Co-P-B/Ni is dipped in MeOH solution of AB. Thus, AB loaded with THF solution was further used for the H_2 generation measurement by thermolysis reaction.

Dehydrogenation temperature and release of volatile gases from neat AB powder and AB loaded over Co-P-B/Ni catalyst were studied by TPDS in the temperature range of 50–200 °C with heating rate of 2 °C/min: results are reported in Fig. 7. As expected, for neat AB two broad H_2 peaks centered at 110 and 165 °C are observed signaling two steps release of H_2 gas with formation of polyaminoborane $(NH_2BH_2)_n$ and polyiminoborane $(NHBH)_n$, respectively. On the contrary, the AB loaded on Co-P-B/Ni catalyst releases first mole of H_2 at considerably lower temperature starting at 50 °C and with the broad desorption peak centered at 80 °C (30 °C lower than that of neat AB) while second peak of H_2 evolves at only 125 °C with lower intensity as compared to neat AB. To our best of knowledge, the dehydrogenation temperature value reported for the present Co-P-B catalyst coating, for first mole of H_2, is the lowest reported for solid state catalyst as summarized in Table 1. The temperature value is much lower than that reported for metallic catalyst like NiPt alloy hollow spheres, Co, Ni, and Cu based salt. Only boron nitride showed dehydrogenation temperature lower than Co-P-B catalyst

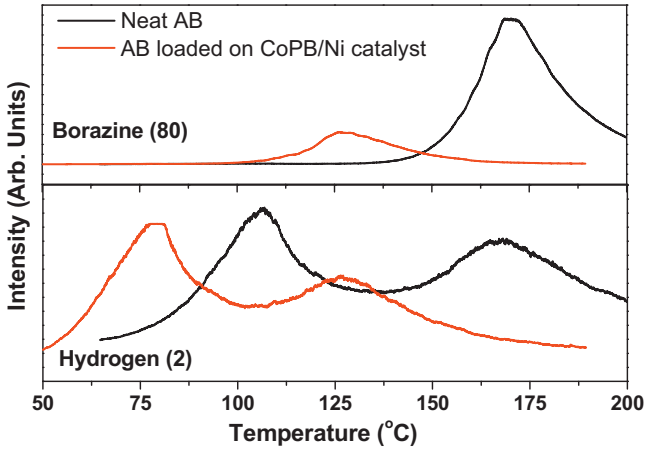

Fig. 7. TPDS/MS profiles of neat AB powder and AB loaded over Co-P-B/Ni catalyst, by using THF based solution. The scanned temperature was between 50 °C and 200 °C at heating rate of 2 °C/min. The hydrogen and borazine with atomic mass of 2 and 80, respectively, have been highlighted in the figure.

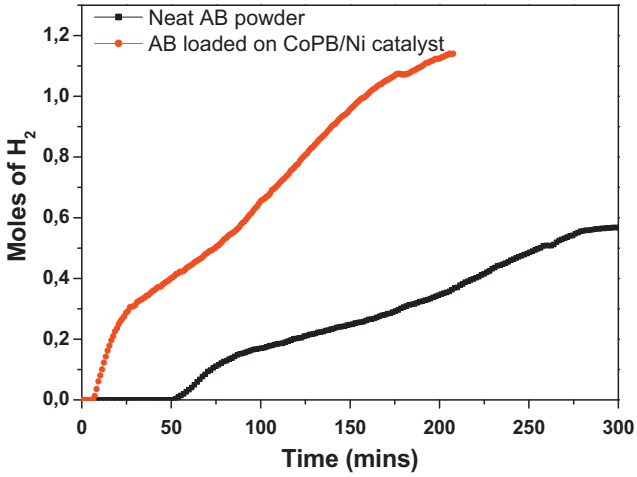

Fig. 8. Volumetric hydrogen production by thermolysis of neat AB powder and AB loaded on Co-P-B/Ni catalyst at 85 °C.

Table 1
Comparison of peak temperature values for release of first mole of H_2 for different solid state catalysts reported in the literature.

Solid state catalysts	Peak temperature for release of first mole of H_2 (°C)
Nanoscaffold silica [19]	95
Metal-organic framework [20]	84
Carbon cryogel [22]	90
Boron nitride [23]	70
Poly(methylacrylate) [27]	95
$Ni_{1-x}Pt_x$ [28]	100
$CuCl_2$, $CoCl_2$, $NiCl_2$ [26]	90
Co-P-B/Ni catalyst [present]	80

but by using AB:catalyst ratio of 1:4 and the amount of borazine formed is several times higher than neat AB. Furthermore, by using the present catalyst the release of borazine gas, a major impurity in decomposition of AB, is significantly lower (6 times) as compared to the neat AB. Ammonia gas content was below detection limit for AB loaded Co-P-B/Ni catalyst coating.

The above result suggests that in presence of catalyst the dehydrogenation of AB follows different paths to release H_2 gas at low temperature. The thermal dehydrogenation of neat AB mainly occurs by induction, nucleation, and growth route. The induction period is mainly due to the formation of diamoniate diborane (DADB) which initiates the dehydrogenation reaction to release H_2 gas [48]. The longer the formation time of DADB, the higher the onset temperature of AB decomposition. However, in presence of metallic catalyst the detailed mechanism is still unclear but the enhanced effect can be due to the metal sites which act as Lewis acid sites and initiate the reaction by oxidation of a B–H bond (at the metal catalyst) which may influence the polar N–H bonds followed by β-H elimination from nitrogen to release H_2 and H_2NBH_2 [49]. With the present catalyst, the synergic effects caused by P and B create high number of electron-enriched Co metal active sites which provide ideal conditions to form Co-H-B intermediate. This catalytic dehydrogenation starts before the melting point of AB thus minimizing the formation of byproduct such as borazine which is mainly formed after melting of AB. The interaction between metal site and $-BH_3$ may also strengthen the N–B bond to prevent the NH_3 formation [22]. The catalyst coating morphology exhibiting nanoflakes with sharp edges of few nanometers might also contribute to reduce the dehydrogenation temperature by acting as nucleation sites.

Gas volumetric method is used to further examine the thermal decomposition properties of AB samples loaded on catalyst coating. Fig. 8 presents the comparison between neat AB powder and AB loaded on Co-P-B/Ni catalyst for H_2 production by thermolysis reaction at 85 °C (working temperature of fuel cell). The AB:Co-P-B catalyst ratio used for the measurement was around 7:1. The neat AB requires around 55 min to initiate the reaction at 85 °C and even after 5 h it is able to produce only 0.6 mol of hydrogen. In contrast, the induction time for AB loaded over catalyst coating is about 7 min at 85 °C which is mainly due to the time required to attain the set temperature over catalyst. Approximately 1.1 mol of H_2 is released within 200 min. The long induction time observed for the neat AB is due to the time required for the formation of initiator in form of DADB [48]. In the case of catalyst induced dehydrogenation, it may be suggested that the interaction between Co nucleation sites (on the nano-flakes) and AB disrupts the dihydrogen bonding (B–H···H–N) in AB molecules at the catalyst–AB interface. Later, by chain reaction the whole network of the dihydrogen bond is destabilized to reduce the induction period of AB decomposition [48]. The H_2 generation rate is about 5 times higher for AB with catalyst as compared to neat AB: this proves the efficient nature of the Co-P-B catalyst mainly established by Co active sites created by synergic effects of B and P elements.

The amounts of H_2, measured through thermolysis reaction for neat AB powder and AB loaded over catalyst coating, as a function of time at different reaction temperatures, are reported in Figs. 9 and 10 respectively. The Arrhenius plot of the hydrogen production rate gives an activation energy value of 134 ± 1 kJ mol^{-1} for AB loaded over Co-P-B coating (inset of Fig. 10) which is significantly lower than that obtained with neat AB powder (179 ± 1 kJ mol^{-1}) (inset of Fig. 9). The obtained low value of energy barrier again proves that thermolysis of AB in presence Co-P-B/Ni catalyst follows different routes with respect to neat AB, while synergic effects caused by B and P elements in the catalyst create favorable condition for H_2 release.

The above results show that the Co-P-B catalyst deposited on Ni foam by ED is highly efficient, not expensive, and can be used for both hydrolysis as well as thermolysis reaction of AB. Another important characteristic of the present catalyst is that it can be effortlessly deposited on any kind of substrate or catalyst bed with relevant advantage that it can be recovered and reused thus being suitable to act as ON/OFF switch to control hydrolysis reaction. Furthermore, even in thermolysis reaction the product mixture may be easily separated by dispersing it in alcohol to collect the undissolved Co-P-B/Ni foam catalyst thus having the advantage to be recovered and used several times.

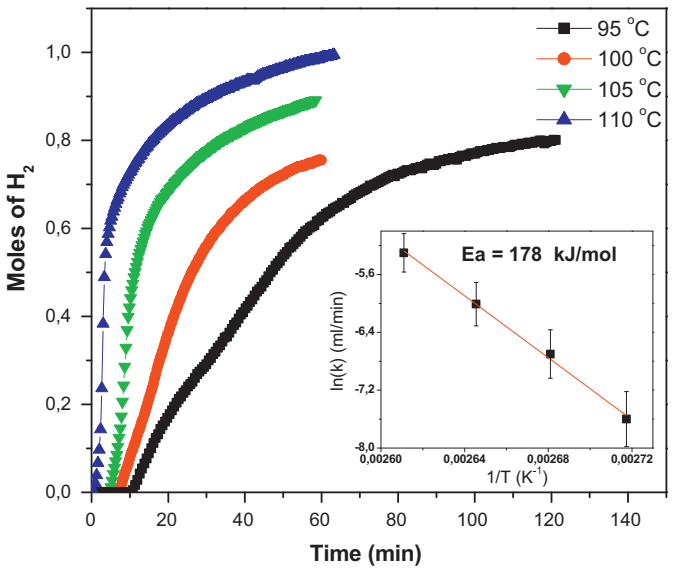

Fig. 9. Volumetric hydrogen production by thermolysis of neat AB powder at different temperatures. Inset shows the Arrhenius plot of the H_2 generation rates to obtain activation energy.

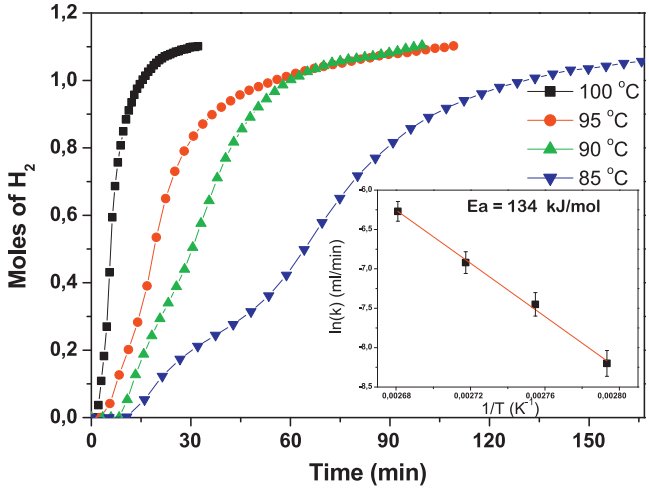

Fig. 10. Volumetric hydrogen production by thermolysis of AB loaded on Co-P-B/Ni catalyst at different temperatures. Inset shows the Arrhenius plot of the H_2 generation rates to obtain activation energy.

4. Conclusions

Co-P-B catalyst coating, synthesized on Ni-foam by using ED, was investigated on catalytic dehydrogenation (both hydrolysis and thermolysis) of AB for H_2 generation and compared to powder Co-P-B catalyst. XPS analysis of the catalyst permitted to establish that: (1) there is electron transfer from alloying B to vacant d-orbital of metallic Co thus making B electron deficient and Co enriched with electrons; (2) the role of P in the Co-P-B catalyst is to favor the enrichment of the surface with Co active sites. Both points (1) and (2) are synergic in increasing efficiency of the Co-P-B catalyst.

In hydrolysis reaction, catalyst coating shows superior catalytic activity as compared to Co-B powder, with complete evolution of H_2 (97%) at very high rate (2 l/min/g catalyst). In thermolysis reaction, AB loaded on Co-P-B/Ni catalyst releases first mole of H_2 starting at 50 °C with desorption peak centered around to 80 °C. To our knowledge, this temperature value is the lowest reported for solid state catalyst in thermolysis reaction of AB. In addition, there is not induction time in the catalytic thermolysis while formation of undesirable byproduct like borazine and ammonia is minimized. Finally, the Co-P-B/Ni coating may be easily recovered and reused.

Acknowledgements

We thank N. Bazzanella for SEM-EDS analysis, C. Armellini for XRD analysis, and S. Torrengo for XPS analysis.

References

[1] L. Zhou, Renew. Sust. Energ. Rev. 9 (2005) 395.
[2] B. Peng, J. Chen, Energy Environ. Sci. 5 (2008) 479.
[3] U.B. Demirci, P. Miele, Energy Environ. Sci. 2 (2009) 627.
[4] Q. Xu, M. Chandra, J. Alloys Compd. 446 (2007) 729.
[5] M. Chandra, Q. Xu, J. Power Sources 156 (2006) 190.
[6] S. Basu, A. Brockman, P. Gagare, Y. Zheng, P.V. Ramachandran, W.N. Delgass, J.P. Gore, J. Power Sources 188 (2009) 238.
[7] V.I. Simagina, P.A. Storozhenko, O.V. Netskina, O.V. Komova, G.V. Odegova, Y.V. Larichev, A.V. Ishchenko, A.M. Ozerova, Catal. Today 138 (2008) 253.
[8] N. Mohajeri, A. T-Raissi, O. Adebiyi, J. Power Sources 167 (2007) 482.
[9] Ö. Metin, S. Sahin, S. Özkar, Int J. Hydrogen Energy 34 (2009) 6304.
[10] F. Durap, M. Zahmakiran, S. Özkar, Int J. Hydrogen Energy 34 (2009) 7223.
[11] M. Zahmakiran, S. Özkar, Appl. Catal. B: Environ. 89 (2009) 104.
[12] T. Umegaki, J.M. Yan, X.B. Zhang, H. Shioyama, N. Kuriyama, Q. Xu, J. Power Sources 195 (24) (2010).
[13] Q. Xu, M. Chandra, J. Power Sources 163 (2006) 364.
[14] Ö. Metin, S. Özkar, Energy Fuel 23 (2009) 3517.
[15] T.J. Clark, G.R. Whittell, I. Manners, Inorg. Chem. 46 (2007) 7522.
[16] J.M. Yan, X.B. Zhang, H. Shioyama, Q. Xu, J. Power Sources 195 (4) (2010) 1091.
[17] T. Umegaki, J.M. Yan, X.B. Zhang, H. Shioyama, N. Kuriyama, Q. Xu, Int. J. Hydrogen Energy 34 (2009) 3816.
[18] J.M. Yan, X.B. Zhang, S. Han, H. Shioyama, Q. Xu, Angew. Chem. Int. Ed. 47 (2008) 2287.
[19] C.F. Yao, L. Zhuang, Y.L. Cao, X.P. Ai, H.X. Yang, Int. J. Hydrogen Energy 33 (2008) 2462.
[20] T. Umegaki, J.M. Yan, X.B. Zhang, H. Shioyama, N. Kuriyama, Q. Xu, J. Power Sources 191 (2009) 209.
[21] A. Gutowska, L. Li, Y.S. Shin, C.M. Wang, X.H.S. Li, J.C. Linehan, R.S. Smith, B.D. Kay, B. Schmid, W. Shaw, M. Gutowski, T. Autrey, Angew. Chem. Int. Ed. 44 (2005) 3578.
[22] Z. Li, G. Zhu, G. Lu, S. Qiu, X. Yao, J. Am. Chem. Soc. 132 (2010) 1490.
[23] M.E. Bluhm, M.G. Bradley, R. Butterick, U. Kusari, L.G. Sneddon, J. Am. Chem. Soc. 128 (2006) 7748.
[24] A. Feaver, S. Sepehri, P. Shamberger, A. Stowe, T. Autrey, G. Cao, J. Phys. Chem. B 111 (2007) 7469.
[25] D. Neiner, A. Karkamkar, J.C. Linehan, B. Arey, T. Autrey, S.M. Kauzlarich, J. Phys. Chem. C 113 (2009) 1098.
[26] X. Kang, Z. Fang, L. Kong, H. Cheng, X. Yao, G. Lu, P. Wang, Adv. Mater. 20 (2008) 2756.
[27] R.J. Keaton, J.M. Blacquiere, R.T. Baker, J. Am. Chem. Soc. 129 (2007) 1844.
[28] S.B. Kalidindi, J. Joseph, B.R. Jagirdar, Energy Environ. Sci. 2 (2009) 1274.
[29] J. Zhao, J. Shi, X. Zhang, F. Cheng, J. Liang, Z. Tao, J. Chen, Adv. Mater. 22 (2010) 394.
[30] F. Cheng, H. Ma, Y. Li, J. Chen, Inorg. Chem. 46 (2007) 788.
[31] R. Fernandes, N. Patel, A. Miotello, Appl. Catal. B: Environ. 92 (2009) 68.
[32] N. Patel, G. Guella, A. Kale, A. Miotello, B. Patton, C. Zanchetta, L. Mirenghi, P. Rotolo, Appl. Catal. A: Gen. 323 (2007) 18.
[33] R. Fernandes, N. Patel, A. Miotello, M. Filippi, J. Mol. Catal. A: Chem. 298 (2009) 1.
[34] N. Patel, R. Fernandes, A. Miotello, J. Power Sources 188 (2009) 411.
[35] R. Fernandes, N. Patel, A. Miotello, Int. J. Hydrogen Energy 34 (2009) 2893.
[36] N. Patel, R. Fernandes, G. Guella, A. Kale, A. Miotello, B. Patton, C. Zanchetta, J. Phys. Chem. C 112 (2008) 6968.
[37] C. Zanchetta, B. Patton, G. Guella, A. Miotello, Meas. Sci. Technol. 18 (2007) N21.
[38] R. Checchetto, L.M. Gratton, A. Miotello, C. Cestari, Meas. Sci. Technol. 6 (1995) 1605.
[39] N. Patel, R. Fernandes, N. Bazzanella, A. Miotello, Thin Solid Films 518 (2010) 4779.
[40] A. Baiker, Faraday Discuss. Chem. Soc., 87 (1989) 239.
[41] W.L. Dai, M.H. Qiao, J.F. Deng, Appl. Surf. Sci. 120 (1997) 119.
[42] A. Lebugle, U. Axelsson, R. Nyholm, N. Martensson, Phys. Scripta 23 (1981) 825.
[43] B.H. Liu, Q. Li, Int. J. Hydrogen Energy 33 (2009) 7385.
[44] H. Li, H.X. Li, W.L. Dai, Z. Fang, J.F. Deng, Appl. Surf. Sci. 152 (1999) 25.
[45] H. Li, Y. Wu, H. Luo, M. Wang, Y. Xu, J. Catal. 214 (2003) 15.
[46] N. Patel, R. Fernandes, G. Guella, A. Miotello, Appl. Catal. B: Environ. 95 (2010) 137.
[47] H.B. Dai, L.L. Gao, Y. Liang, X.D. Kang, P. Wang, J. Power Sources 195 (2010) 307.
[48] R. Benzouaa, U.B. Demirci, R. Chiriac, F. Toche, P. Miele, Thermochim. Acta 509 (2010) 81.
[49] N.C. Smythe, J.C. Gordon, Eur. J. Inorg. Chem. 509 (2010).